International Journal of Thermodynamics (IJoT)
ISSN 1301-9724 / e-ISSN 2146-1511
https://dergipark.org.tr/en/pub/ijot

Vol. xx (No. x), pp. xxx-xxx, 2025
doi: 10.5541/ijot.1514519
Published online: Mmm dd, 2025

Research Article

Exergetic Evaluation of Heat Exchanger with Multiple Inserts for Greenhouse Heating

[1]M. Kumar, [1*]A. K. Patil

[1] Department of Mechanical Engineering, DIT University, Dehradun-248009, Uttarakhand, India
E-mail: [1*]dr.anilpatil@dituniversity.edu.in

Received 11 July 2024, Revised 30 August 2024, Accepted 04 October 2024

Abstract

The heat exchanger performance is vital for attaining higher overall performance of the greenhouse heating system. The exergetic performance is evaluated for the heat exchanger using twisted tape inserts for greenhouse heating. Single, a set of two, and four twisted tapes of TR 2.5-3.5 are considered for the analysis by varying Reynolds number (Re) from 3000 to 15000. A set of two twisted tapes causes a decrease in total entropy generation up to Re of 7650 and increases beyond this value. The maximum and minimum values of the Bejan number are obtained for the smooth tube and the tube with twisted tapes (four) in "counter-swirl" orientation, respectively. The twisted tapes are feasible under the Reynolds number of 9042 based on the analysis of the entropy generation number. The minimum value of total entropy generation is obtained as 0.00035 for the four twisted tapes in counter-swirl orientation (FTT-COUS). The maximum exergy efficiency is observed for a twisted tape insert at a pitch ratio of 3.5.

Keywords: *Twisted tapes; twist ratio; entropy generation; exergy; reynolds number.*

1. Introduction

Modern farming requires a significant amount of thermal energy for greenhouse heating [1]. The heating costs account for nearly 70-85% of the total cost of energy consumption in greenhouses [2]. Considering the heating expenses, energy-efficient systems need to be used for economic and sustainable greenhouse farming. The heating requirements can be fulfilled from renewable sources like solar, biomass, and geothermal. Attar and Farhat [3] employed capillary heat exchangers for a greenhouse system. By increasing the length by four times, the temperature difference was increased by 1.61 times. Agrebi et al. [4] studied the solar-assisted heat pumps for greenhouse heating. The heating capacity of the solar heat pump was found superior to the ground-coupled heat pump. A coil heat exchanger was introduced in a solar water heating system by Ihoume et al. [5] for greenhouse heating during the winter season. The introduction of a heat exchanger in the greenhouse has increased the night temperature up to 5 ºC. Dhiman et al. [6] investigated the hot water and flue gas heat sink pipe networks supplying hot water and flue gases to the greenhouse for space heating. It was discovered that a temperature difference of 10 °C requires nearly 13 kW of heating load for a 100 m^2 greenhouse area. Aliabadi et al. [7] experimentally studied the thermo-hydraulic performance of a plate fin heat exchanger in a solar heating system. The results showed an improved performance by the application of perforated fins. Boughanmi et al. [8] investigated the greenhouse heating system using a novel geothermal heat exchanger. The conic helicoidally geothermal heat exchanger supplied heat energy to raise the air temperature by 3 °C. The heat exchanger ability significantly affects the greenhouse heating system performance. Usually, active and passive techniques are used to enhance heat transfer in the tubular heat exchanger. Thorsen and Landis [9] reported that the twisted tapes introduce fluid mixing in the tube flow near the walls and thus improved heat transfer. Garcia et al. [10] explored that the wire coil inserts are effective in yielding higher heat transfer rates in the transitional flow regime. Verma et al. [11] found a better performance of modified helical coiled inserts over conventional wire coil inserts in a tubular flow. Wang et al. [12] employed multiple pairs of longitudinal vortexes in a tube passage. The longitudinal vortexes were better suited in a laminar flow regime. Abdolbaqi et al. [13] explored the effects of twin twisted tapes in two different orientations. The "counter-swirl" twin tapes were found effective in enhancing heat transfer. Chang et al. [14] used single, double, and triple twisted tapes in a flow-through circular tube for heat transfer augmentation. It was observed that the heat transfer rates of double and triple-twisted tapes were better than a single twisted tape. Vashistha et al. [15] used multiple twisted tape inserts in flow through a circular tube for thermo-hydraulic analysis. The most effective thermo-hydraulic performance was shown by four "counter-swirl" twisted tapes.

In a study by Badji et al. [16], the cost and energy consumption depends on the geometry, orientation, and covering material of the greenhouse helps to create a suitable environment for the crop. Naghibi et al. [17] evaluated the role of phase change materials in a solar heating system of a greenhouse. The greenhouse system was improved in terms of energy utilization by 14% using the phase change material. Yıldırım and Gürdal [18] analysed the effect of vortex generator geometry on energy and entropy generation. Taskesen et al. [19] investigated the impact of channel geometry on heat transfer and entropy generation. Cylindrical cross-section of channel produced the maximum heat transfer. Ocak and Karabulut [20] have reported that the lowest entropy generation has been obtained in a pipe with least diameter.

Reviewing existing literature highlights the scope for further performance exploration of the heat exchanger used in greenhouse heating systems for optimum energy utilization. The present study investigates heat exchanger performance based on the second law for one, two, and four twisted tapes in co-swirl / counter-swirl orientations using twist ratio (TR) of 2.5 to 3.5 for Reynolds number range of 3000-15000.

2. Greenhouse Heating System

It consists of a heat exchanger, a pump, and water tanks as shown in Figure 1. The heat exchanger enables the energy transfer between the fluids with the help of a circulating pump. The heat energy may be taken from the heat sources like a solar collector, waste heat from a thermal power plant, exhaust gases, etc. Since the heat exchanger is an important element of the heating system, it is designed to transfer heat with maximum effectiveness. In a tubular heat exchanger, the heat exchange between the two fluids depends on the intervening thermal resistance. In order to reduce the conductive resistance of tube wall, highly conductive material like copper is used for the manufacturing of tubes. However, the convective resistance on two sides of the wall plays a crucial role in achieving the overall heat transfer. Tube inserts are widely used to induce turbulence in the flow and thereby achieving higher heat transfer rates. In the present study, single, double, and four twisted tapes are inserted to enhance the heat transfer rate. The double and four twisted tapes are employed in two orientations, i.e., "co-swirl" and "counter-swirl". The twisted tapes are shown in Figure 2. The experimental data has been collected using the heat exchanger test rig reported by Vashistha et al. [15]. The test section consists of a copper tube having diameter 25 mm and length 1000 mm. During the experimental test run, the twisted tapes were inserted centrally along the entire length of the test section. Twisted tape in the tube induces swirl motion by which the fluid gets heated by taking energy from the tube surface. It was uniformly heated by providing the heat flux from the outer surface of the tube. The test section of heat exchanger is insulated using glass wool and insulating foam to minimize the environmental effects. The measurements such as temperature of the test section, temperature of water at inlet and outlet, pressure drop across the test section, and the flow rate were recorded under the steady-state conditions.

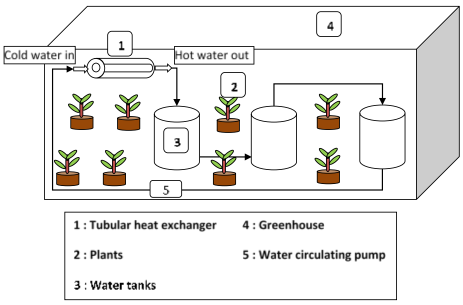

Figure 1. Schematic arrangement of a greenhouse heating system.

Figure 2. Twisted tapes (twist ratio 3.5, 3, and 2.5).

Table 1. Variable tape parameters.

Types of inserts	Twist ratio
Single twisted tape (STT)	2.5, 3, 3.5
Twin twisted tapes in co-swirl orientation (TTT-COS)	2.5, 3, 3.5
Twin twisted tapes in counter-swirl orientation (TTT-COUS)	2.5, 3, 3.5
Four twisted tapes in co-swirl orientation (FTT-COS)	2.5, 3, 3.5
Four twisted tapes in counter-swirl orientation (FTT-COUS)	2.5, 3, 3.5

3. Performance Parameters

Heat transfer to the greenhouse by using the working fluid is estimated as:

$$Q_s = \dot{m}\, C_p \left(T_s - T_g\right) \quad (1)$$

Under the adiabatic condition, the energy transfer in heat exchanger is same as from storage tanks to the greenhouse environment, which is given as:

$$Q_{HX} = Q_S \quad (2)$$

The rate of heat transfer is quantified as,

$$Q_{HX} = \dot{m}\, C_p (T_o - T_i) \quad (3)$$

The convective rate of heat transfer from the heat exchanger tube surface is given as,

$$Q_{convection} = h\, A_s (T_s - T_b) \quad (4)$$

The mean convective heat transfer coefficient (h) is determined from the energy balance from eq. 3 and 4,

$$h = \frac{\dot{m}\, C_p (T_o - T_i)}{A_s (T_s - T_b)} \quad (5)$$

The mean Nusselt number is determined as:

$$Nu = \frac{hD}{k} \quad (6)$$

The flow Reynolds number in the heat exchanger tube is defined as,

$$Re = \frac{UD}{v} \quad (7)$$

The Darcy-Weisbach friction factor (f) across the heat exchanger is obtained as:

$$f = \frac{2D\,\Delta P}{L\rho U^2} \quad (8)$$

Performance estimation using the II law of thermodynamics needs to determine the entropy generation by thermal and frictional phenomenon [21].

The entropy generation (thermal) is defined as,

$$\dot{S}_{g,t} = \frac{Q^2{}_{convection}}{Nu\,\pi k T_i T_o L} \tag{9}$$

The entropy generation (frictional) is found as [21],

$$\dot{S}_{g,f} = \frac{8 f \dot{m}^3 L}{\rho^2\,\pi^2 D^5 (T_o - T_i)} \ln\left(\frac{T_o}{T_i}\right) \tag{10}$$

Thus, the total entropy generation is [21],

$$\dot{S}_{g,total} = \dot{S}_{g,t} + \dot{S}_{g,f} \tag{11}$$

The Bejan number (B_j) is the ratio of entropy generation (thermal) and the total entropy generation due to thermal and frictional phenomenon, which is given as [21],

$$B_j = \frac{\dot{S}_{g,t}}{\dot{S}_{g,t} + \dot{S}_{g,f}} \tag{12}$$

The entropy generation number (N_e) is given as [21],

$$N_e = \frac{T_{env} \dot{S}_{g,total}}{Q_{convection}} \tag{13}$$

The exergy efficiency (η_{ex}) is the maximum useful energy content in the exergy supplied as shown below [21],

$$\eta_{ex} = 1 - \frac{T_{env} \dot{S}_{g,t}}{\left[1 - \frac{T_{env}}{T_S}\right] Q_{convection}} \tag{14}$$

4. Results and Discussion

To explore the effect of inserting twisted tapes on a greenhouse heat exchanger performance, a second law thermodynamic analysis was carried out. Entropy generation for thermal energy transfer and frictional heating is separately evaluated for different combinations of twisted tapes to understand their effects. A combined effect of these inserts is also observed by evaluating the total entropy generation. The Bejan number quantifies the entropy generation by thermal energy transfer which accounts for exergy losses by inserts.

The entropy generation number signifies the dimensionless exergy losses relative to the energy supplied to the system. Lower values of entropy generation number are preferred while designing an effective heat transfer system. The thermodynamic analysis concludes with the determination of exergetic efficiency of the system which is a measure of how effectively, the input exergy is utilized by the system.

Figure 3 shows the variation of entropy generation (thermal) using twisted tape inserts. It is evident from the plot that the smooth tube without any insert generates maximum thermal entropy regardless of the Reynolds number and thus it is unsuitable for the intended application. As the Reynolds number increases, the entropy generation (thermal) declines in all cases. Further, the entropy generation (thermal) is reduced in the order of a twisted tape, "co-swirl" oriented twisted tapes (two), "counter-swirl" oriented twisted tapes (two), "co-swirl" oriented twisted tapes (four), and "counter-swirl" oriented twisted tapes (four). Furthermore, reducing twist ratios of tapes in each category reduces entropy generation. A combination of "counter-swirl" oriented twisted tapes (four) yields entropy generation (thermal).

The twisted tape brings swirl motion in the fluid stream which promotes turbulence in the boundary layer. Twisted tape induced turbulence promotes mixing of fluid layers which reduces entropy generation due to finite temperature difference. Twin twisted tapes further promote the fluid mixing as a result of their individual vortices moving in same or opposite direction and thereby decrease the entropy generation. The effect of co-swirl and counter-swirl vortices is different: co-swirl motion creates thermally inactive zones whereas the counter-swirl motion intensify fluid mixing. Four twisted tapes generate four vortices along with two impingement zones. The multiple vortices energize the boundary layer flow with a suppression of viscous effects by the flow impingements. The thermal irreversibility is settled to the minimum level due to these notable changes in the fluid flow.

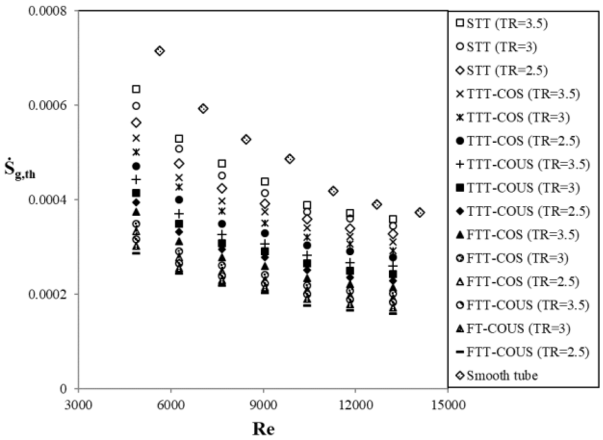

Figure 3. Entropy generation (thermal) vs Re.

Figure 4 shows the entropy generation (frictional) for different twisted tapes. The maximum entropy generation (frictional) is observed for "counter-swirl" oriented twisted tapes (four). The entropy generation (frictional) ascends with the Reynolds number. Further, the entropy generation (frictional) declines in the order of "counter-swirl" oriented four twisted tapes, "co-swirl" oriented four twisted tapes, "counter-swirl" oriented twisted tapes (two), "co-swirl" oriented twisted tapes (two), single twisted tape, and smooth tube. The intensity of turbulence in the flow field is proportional to the frictional losses which is responsible for the entropy generation. The entropy generation escalates with the frictional losses in the order of single twisted tape, twin twisted tapes, and four twisted tapes.

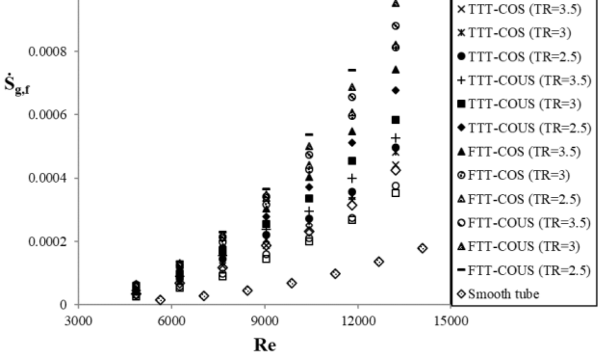

Figure 4. Entropy generation (frictional) vs Re.

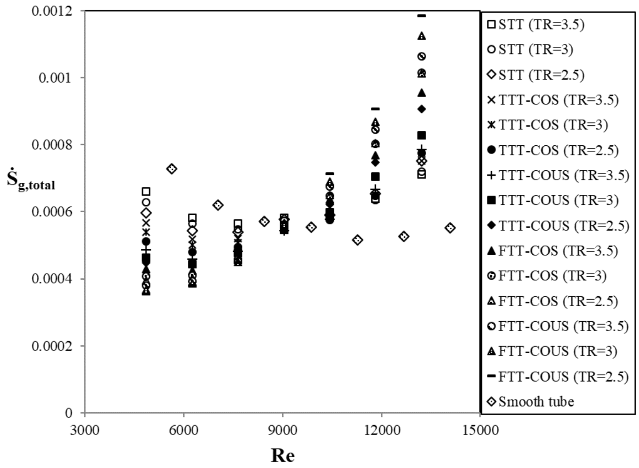

Figure 5. Total entropy generation vs Re.

The entropy generation (total) trends for the heat exchanger tube using twisted tape inserts are depicted in Figure 5. For a smooth tube, the total entropy generation declines with the Reynolds number. However, twisted tapes (four) in both orientations bring higher entropy generation with increasing Reynolds number. A slightly different trend is observed in twisted tapes (two) with "co-swirl" and "counter-swirl" orientations, for which, the entropy generation initially decreases up to the Reynolds number of 7650 and increases afterward. Whereas in a single twisted tape insert, the entropy generation initially decreases up to the Reynolds number of 6260 increases afterward. The analysis of total entropy generation reveals that the combination of twisted tapes (four) should be preferred at a lower Reynolds number whereas single and twisted tapes (two) are performing better at around the Reynolds number of 7650.

The minimum value of total entropy generation for smooth tube and tube with different tapes is reported in Table 2.

Table 2. Minimum entropy generation.

Type of inserts	Minimum value of Total entropy generation ($\dot{S}_{g,total}$) (W/K)		
	TR=2.5	TR=3	TR=3.5
Smooth tube		0.00052	
Single twisted tape (STT)	0.00054	0.00055	0.00056
Twin twisted tapes in co-swirl Orientation (TTT-COS)	0.00048	0.00050	0.00052
Twin twisted tapes in counter-swirl orientation (TTT-COUS)	0.00044	0.00044	0.00046
Four twisted tapes in co-swirl orientation (FTT-COS)	0.00040	0.00041	0.00042
Four twisted tapes in counter-swirl orientation (FTT-COUS)	0.00035	0.00037	0.00038

Bejan number reduces at a particular Reynolds number by the application of twisted tapes, and as the number of twisted tape inserts increases, the reduction is even greater. This observation confirms the lower entropy generation (frictional) and higher entropy generation (thermal) by a single twisted tape. As twisted tapes are increased, the entropy generation (thermal) declines at the cost of increased entropy generation (frictional). The "counter-swirl" orientation of twisted tapes in a set of two and four inserts shows a lower Bejan number compared to "co-swirl" orientations. The minimum value of the Bejan number corresponds to "counter-swirl" oriented twisted tapes (four).

The entropy generation in a thermodynamic process is also evaluated by using the entropy generation number representing exergy destruction in a process. Figure 7 shows the plot of the entropy generation number with and without twisted tapes. It is found that the application of twisted tapes is feasible under the Reynolds number of 9042. Further, an increase in the number of twisted tapes leads to a declining entropy generation number. It also decreases as the twist ratio is reduced and favours the "counter-swirl" orientation.

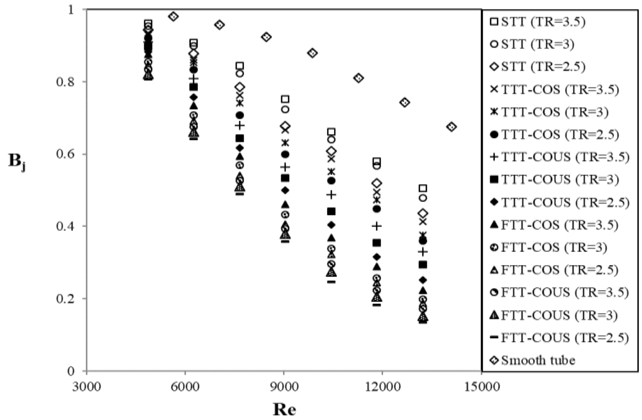

Figure 6. Bejan number vs Re.

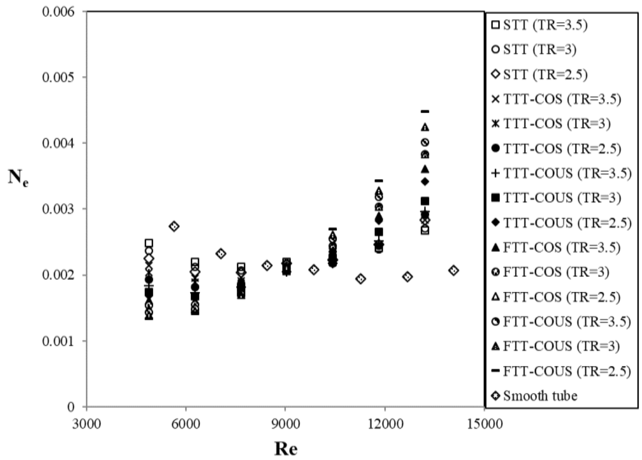

Figure 7. Entropy generation number vs Re.

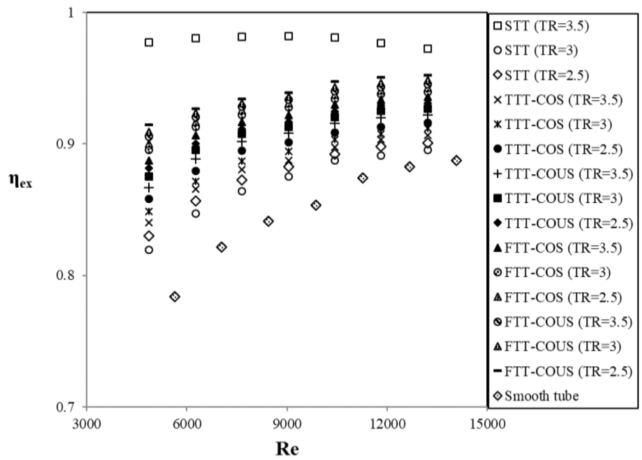

Figure 8. Exergy efficiency vs Re.

The exergy efficiency for different twisted tapes is evaluated in Figure 8. The maximum exergy efficiency is attained by a single twisted tape insert at a pitch ratio of 3.5. whereas the minimum exergy efficiency is observed for a smooth tube. An increase in exergy efficiency is observed in all cases except a single twisted tape insert at a pitch ratio of 3.5, which is marginally affected by the change in Reynolds number. The twisted tapes (four) with "counter-swirl" orientation having a pitch ratio of 2.5 appear to be the best-performing geometry after STT (y=3.5).

5. Conclusions

The present study presents the results of the thermodynamic performance evaluation of a heat exchanger used in the greenhouse heating system. The entropy generation by thermal and fluid friction was evaluated for Re of 3000-15000. The performance of heat exchanger using twisted tapes was gauged by Bejan number, entropy generation number, and exergy efficiency. Based on the analysis of results, the following notable outcomes are reported:

- With the increasing number of twisted tapes, entropy generation (thermal) is diminished. The minimum entropy generation (thermal) corresponds to "counter-swirl" oriented twisted tapes (four). Frictional losses generate more entropy as Reynolds number increases. The maximum entropy generation (frictional) is observed for "counter-swirl" oriented twisted tapes (four).
- The total entropy generation declines for a smooth tube and increases for twisted tapes (four) as Re is increased.
- The total entropy generation initially decreases up to Re of 7650 and increases beyond this value for two twisted tapes.
- Bejan number declines at a higher Reynolds number without any exception. The smooth tube has a maximum value of Bejan number. The minimum value of the Bejan number is observed for "counter-swirl" oriented twisted tapes (four).
- The analysis of the entropy generation number shows that the feasible range of the Reynolds number is below 9042 for twisted tape application.
- The maximum exergy efficiency is observed for a twisted tape at a pitch ratio of 3.5.

Conflict of Interest

Authors approve that to the best of their knowledge, there is not any conflict of interest or common interest with an institution/organization or a person that may affect the review process of the paper.

Nomenclature

A	*Area*	m^2
Bj	*Bejan number*	-
C_p	*Specific heat at constant pressure*	*J/kg K*
D	*Tube diameter*	*m*
f	*Friction factor*	-
h	*Convection heat transfer coefficient*	$W/m^2\ K$
k	*Thermal conductivity*	*W/m K*
L	*Length of the tube*	*m*
$\dot{m}$	*Mass flow rate*	*kg/s*
Nu	*Nusselt number*	-
N_e	*Entropy generation number*	-
P	*Pitch*	*mm*
Δp	*Pressure difference across tube*	N/m^2
Q	*Heat transfer rate*	*W*
Re	*Reynolds number*	-
T	*Temperature*	*K*
U	*Mean velocity of fluid*	*m/s*
y	*Twist ratio*	-
Greek Symbols		
ν	*Kinematic Viscosity of fluid*	m^2/s
ρ	*Density of fluid*	kg/m^3
η_{ex}	*Exergy efficiency*	-
Subscripts		
b	*Bulk*	-
env	*Environmental*	-
g	*Greenhouse*	-
g,t	*Generation-thermal*	-
g,f	*Generation-frictional*	-
g,total	*Generation-total*	-
HX	*Heat exchanger*	-
i	*Inlet*	-
o	*Outlet*	-
s	*Surface*	-

References:

[1] M. S. Ahamed, H. Guo, and K. Tanino, "Energy saving techniques for reducing the heating cost of conventional greenhouses," *Biosystems Engineering*, vol. 178, pp. 9–33, 2019, doi: 10.1016/j.biosystemseng.2018.10.017.

[2] A. S. Anifantis, A. Colantoni, and S. Pascuzzi, "Thermal energy assessment of a small scale photovoltaic, hydrogen and geothermal stand-alone system for greenhouse heating," *Renewable Energy*, vol. 103, pp. 115–127, 2017, doi: 10.1016/j.renene.2016.11.031.

[3] I. Attar and A. Farhat, "Efficiency evaluation of a solar water heating system applied to the greenhouse climate," *Solar Energy*, vol. 119, pp. 212–224, 2015, doi: 10.1016/j.solener.2015.06.040.

[4] S. Agrebi, R. Chargui, B. Tashtoush, and A. A. Guizani, "Comparative performance analysis of a solar assisted heat pump for greenhouse heating in Tunisia," *International Journal of Refrigeration*, vol. 131, pp. 547–558, 2021, doi: 10.1016/j.ijrefrig.2021.06.004.

[5] I. Ihoume, R. Tadili, N. Arbaoui, A. Bazgaou, A. Idrissi, M. Benchrifa, and H. Fatnassi, "Performance study of a sustainable solar heating system based on a copper coil water to air heat exchanger for greenhouse heating," *Solar Energy*, vol. 232, pp. 128–138, 2022, doi: 10.1016/j.solener.2021.12.064.

[6] M. Dhiman, V. P. Sethi, B. Singh, and A. Sharma, "CFD analysis of greenhouse heating using flue gas and hot water heat sink pipe networks," *Computers and Electronics in Agriculture*, vol. 163, 2019, Art. no. 104853, doi: 10.1016/j.compag.2019.104853.

[7] M. Khoshvaght-Aliabadi, M. Tatari, and M. Salami, "Analysis on Al_2O_3/water nanofluid flow in a channel by inserting corrugated/perforated fins for solar heating heat exchangers," *Renewable Energy*, vol. 115, pp. 1099–1108, 2018, doi: 10.1016/j.renene.2017.08.092.

[8] H. Boughanmi, M. Lazaar, and A. Guizani, "A performance of a heat pump system connected a new

conic helicoidal geothermal heat exchanger for a greenhouse heating in the north of Tunisia," *Solar Energy*, vol. 171, pp. 343–353, 2018, doi: 10.1016/j.solener.2018.06.054.

[9] R. Thorsen and F. Landis, "Friction and heat transfer characteristics in turbulent swirl flow subjected to large transverse temperature gradients," *Journal of Heat Transfer*, vol. 90, pp. 87–97, 1968, doi: 10.1115/1.3597466.

[10] A. García, J. P. Solano, P. G. Vicente, and A. Viedma, "Enhancement of laminar and transitional flow heat transfer in tubes by means of wire coil inserts," *International Journal of Heat and Mass Transfer*, vol. 50, pp. 3176–3189, 2007, doi: 10.1016/j.ijheatmasstransfer.2007.01.015.

[11] A. Verma, M. Kumar, and A. K. Patil, "Enhanced heat transfer and frictional losses in heat exchanger tube with modified helical coiled inserts," *Heat and Mass Transfer*, vol. 54, pp. 3137–3150, 2018, doi: 10.1016/j.ijheatmasstransfer.2007.01.015.

[12] Y. Wang, P. Liu, F. Shan, Z. Liu, and W. Liu, "Effect of longitudinal vortex generator on the heat transfer enhancement of a circular tube," *Applied Thermal Engineering*, vol. 148, pp. 1018–1028, 2019, doi: 10.1016/j.applthermaleng.2018.11.080.

[13] M. K. Abdolbaqi, W. H. Azmi, R. Mamat, N. M. Z. N. Mohamed, and G. Najafi, "Experimental investigation of turbulent heat transfer by counter and co-swirl flow in a flat tube fitted with twin twisted tapes," *International Communications in Heat and Mass Transfer*, vol. 75, pp. 295–302, 2016, doi: 10.1016/j.icheatmasstransfer.2016.04.021.

[14] S. W. Chang, K. W. Yu, and M. H. Lu, "Heat transfers in tubes fitted with single, twin, and triple twisted tapes," *Experimental Heat Transfer*, vol. 18, no. 4, pp. 279–294, 2005, doi: 10.1080/08916150500201560.

[15] C. Vashistha, A. K. Patil, and M. Kumar, "Experimental investigation of heat transfer and pressure drop in a circular tube with multiple inserts," *Applied Thermal Engineering*, vol. 96, pp. 117–129, 2016, doi: 10.1016/j.applthermaleng.2015.11.077.

[16] A. Badji, A. Benseddik, H. Bensaha, A. Boukhelifa, and I. Hasrane, "Design, technology, and management of greenhouse: A review," *Journal of Cleaner Production*, vol. 373, 2022, Art. no. 133753, doi: 10.1016/j.jclepro.2022.133753.

[17] Z. Naghibi, R. Carriveau, and D. Ting, "Improving clean energy greenhouse heating with solar thermal energy storage and phase change materials," *Energy Storage*, vol. 2, p. e116, 2020, doi: https://doi.org/10.1002/est2.116.

[18] Y. Furkan and G. Mehmet, "Numerical energy and entropy analyses of a tube with wavy tape insert including $CoFe_2O_4$/water nanofluid under laminar regime," *International Journal of Heat and Fluid Flow*, vol. 108, 2024, Art. no. 109447 doi: 10.1016/j.ijheatfluidflow.2024.109447.

[19] E. Taskesen, M. Tekır, E. Gedik, and K. Arslan, "Numerical investigation of laminar forced convection and entropy generation of Fe_3O_4/water nanofluids in different cross-sectioned channel geometries," *Journal of Thermal Engineering*, vol. 7, no. 7, pp. 1752–1767, 2021, doi: 10.18186/thermal.1025984.

[20] N. Ocak and K. Karabulut, "Entropy and exergy analysis in an experimental thermal system used GO–DW nanofluid having straight copper pipes with different diameters," *Journal of Engineering Thermophysics*, vol. 32, pp. 637–655, 2023, doi: 10.1134/S1810232823030177.

[21] P. G. Kumar, N. Thangapandian, V. S. Vigneswaran, S. Vinothkumar, B. Mouli Prasanth, and S. C. Kim, "Heat transfer, pressure drop, and exergy analyses of a shot-peened tube in the tube heat exchanger using Al_2O_3 nanofluids for solar thermal applications," *Powder Technology*, vol. 401, 2022, Art. no. 117299, doi: 10.1016/j.powtec.2022.117299.